XXXI. SUB-BEAM PRISM OF THE KISO OBSERVATORY

Takeshi NOGUCHI and Takao SOYANO

1. Introduction

Various survey projects have been carried out using a 105-cm Schmidt telescope at the Kiso Observatory (Takase et al. 1977). A lot of interesting objects have been detected through the surveys (e.g. Noguchi et al. 1980, Takase 1980, Noguchi et al. 1983, Takase et al. 1983). Most of them are so faint ($m \gtrsim 15$ mag) that it is very difficult to determine their magnitudes photoelectrically. Thus we are forced to rely on the photographic photometry. Faint standard stars available in the literature are, however, often too few to calibrate the faint objects all over a wide angle plate taken with the Kiso Schmidt telescope. We introduced a new calibration method by means of a sub-beam prism (Noguchi and Soyano 1982; Soyano et al. 1983) in order to calibrate the magnitudes of faint objects using bright standard stars. In the following we present an outline of the prism and its performance.

2. Sub-beam prism

A method of magnitude calibration of faint stars using a sub-beam prism was originally devised by Pickering (1891) and then it was applied to the practical observations by Racine (1969). An application to the Schmidt telescope was reported by Muller (1980). This method makes use of the phenomenon that the light passing through a small prism with a small vertex angle, which is placed in the light path of a telescope, focuses on the point slightly shifted from where the light should focus without the prism, resulting in a secondary image. In the case of the Schmidt telescope it is appropriate that the prism is placed in front of the corrector plate as shown in figure 1. The secondary image produced by the sub-beam prism is fainter than the direct image by the ratio of the aperture of the prism to that of the corrector plate. Thus, the secondary images of the bright standard stars can be used as the supplementary magnitude standards.

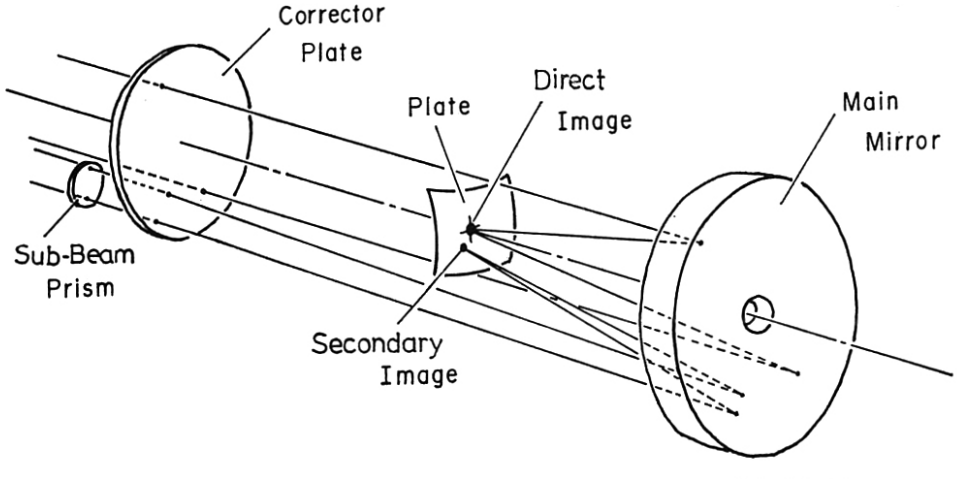

Fig. 1. Optical paths when a sub-beam prism is mounted on the Schmidt telescope.

3. Main characteristics of our sub-beam prism

The sub-beam prism for the Kiso Schmidt telescope is made of the fused quartz and has an aperture of 12 cm and a vertex angle of 88 arcsec. It is amber coated in order to minimize the light loss due to the surface reflection.

The diffraction due to the small aperture of the prism and the chromatic aberration might cause errors in magnitude determination. We estimate the amount of these effects and present the results in tables 1 and 2. As shown in these tables, the effect of the chromatic aberration is

Table 1. Size of the secondary image in various color bands due to diffraction*

Color	U	B	G	V	R	$H\alpha$	I
λ (μm)	0.357	0.438	0.498	0.568	0.644	0.654	0.792
D ($''$)	0.74	0.91	1.04	1.18	1.34	1.36	1.65

* notations λ: effective wave length. D: full width at half maximum of the diffraction image.

Table 2. Chromatic aberrations in various color bands*

Color	U	B	G	V	R	$H\alpha$	I
$\Delta\lambda$ (μm)	0.046	0.086	0.080	0.140	0.084	0.022	0.176
Δn (10^{-4})	52	70	46	54	22	6	25
D ($''$)	0.46	0.62	0.40	0.48	0.20	0.05	0.23

* notations $\Delta\lambda$: band width. Δn: dispersion of the refractive index within the color band. D: image size due to the chromatic aberration.

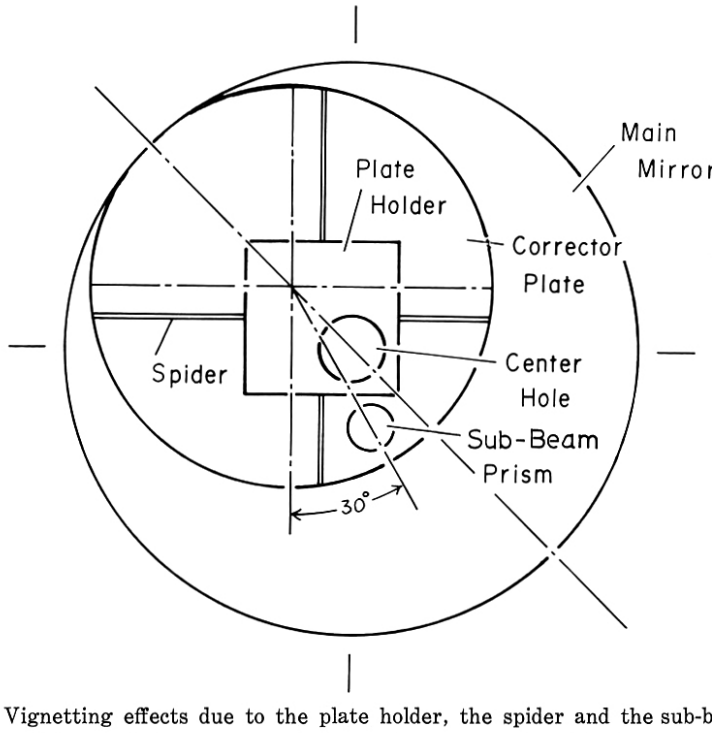

Fig. 2. Vignetting effects due to the plate holder, the spider and the sub-beam prism, projected onto the surface of the main mirror, when the incident light has an inclination of 2 degrees from the optical axis.

negligibly small and make no serious errors. On the other hand the diffraction image due to the small aperture of the prism is about 1 arcsec which is comparable with the seeing size under the good observing condition at the Kiso Observatory. It is desirable that the prism aperture is larger to make the diffraction image smaller. However, an aperture of 12 cm was chosen to give the magnitude difference of 5 mag or more.

The location of the secondary image relative to the direct image is determined by the vertex angle and the direction of the vertex. As shown in figure 2 we mount the prism at the edge of the corrector plate with a position angle of 30 degrees to minimize vignetting due to the plate holder and the spider of plate holder supports. Further the vertex of the prism is set at 22.5 degrees from the north-south direction so that the secondary image does not overlap on diffraction patterns of the plate holder and the spider. Figure 3 shows the sub-beam prism mounted in front of the corrector plate. With this configuration the secondary image produced by the sub-beam prism is located at 44 arcsec south-south-west of the direct image and about 4.5 magnitude fainter than that as shown in figure 4.

A computation shows that vignetting becomes serious for the above configuration at about 2 degrees from the plate center. Thus we have to use the range within a radius of 2 degrees for photometeric works with the sub-beam prism.

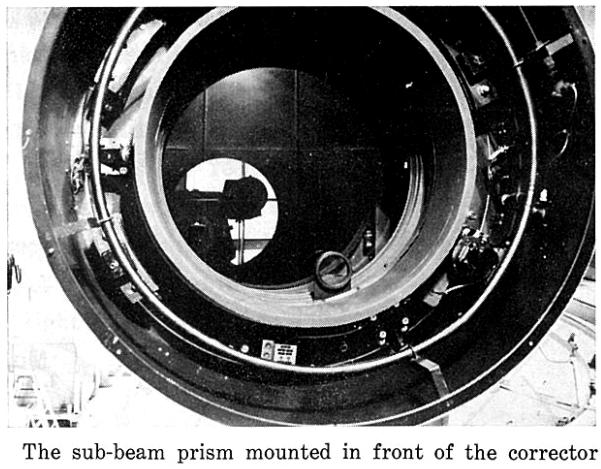

Fig. 3. The sub-beam prism mounted in front of the corrector plate.

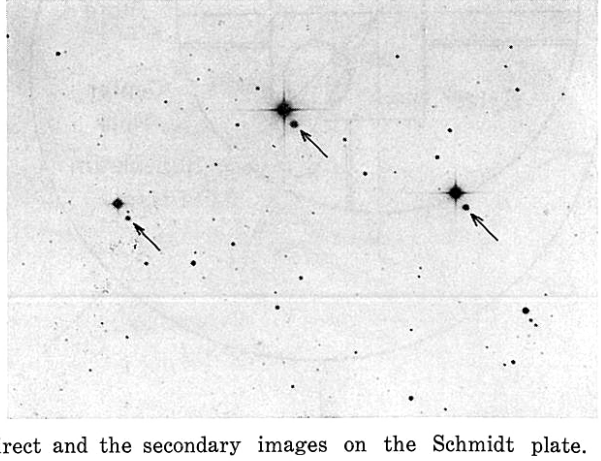

Fig. 4. The direct and the secondary images on the Schmidt plate. The secondary images, which are indicated by arrows, are located at 44 arcsec south-south-west of the direct images.

4. Magnitude difference between the direct and the secondary images.

The magnitude difference between the direct and the secondary images can be calculated from the ratio of the aperture of the sub-beam prism to that of the corrector plate. Taking the vignetting effect into account we estimate the value to be 4.45 magnitude within a radius of 2 degrees from the center.

In order to obtain the actual value of this magnitude difference, we observed a Kiso standard area, which contains the Kapteyn's Selected Area (SA) 57, with the Schmidt telescope. The plates were measured with the iris photometer at the Kiso Observatory (cf. Kiso Information Bulletin, Vol. 1, No. 7, p. 140; Ishida et al. 1978). For the magnitudes of stars in SA 57 the values of Purgathofer (1969) were used. Figure 5 shows an example of a set of the characteristic curves representing the relation between iris readings and B magnitudes of the standard stars for the direct and the secondary images. In figure 6 plotted are the magnitude difference measured in figure 5, ΔM, versus B magnitude. As shown in this figure the magnitude difference obviously depends on the magnitude of the stars. Further experiments show that the slope of this ΔM versus magnitude relation varies from plate to plate.

This dependence of the magnitude difference on the magnitude and its plate-to-plate variation may be due to the difference of the image structure, i.e., the degree of blurring and the amount of incident light, etc., between the direct and the secondary images. The difference of the image structure can be caused by (1) seeing condition or accuracy of focusing and (2) the difference of the chromatic aberration in different color bands. In order to investigate the effects of these two factors on ΔM versus magnitude relation, we took several plates in U, B and V color bands under

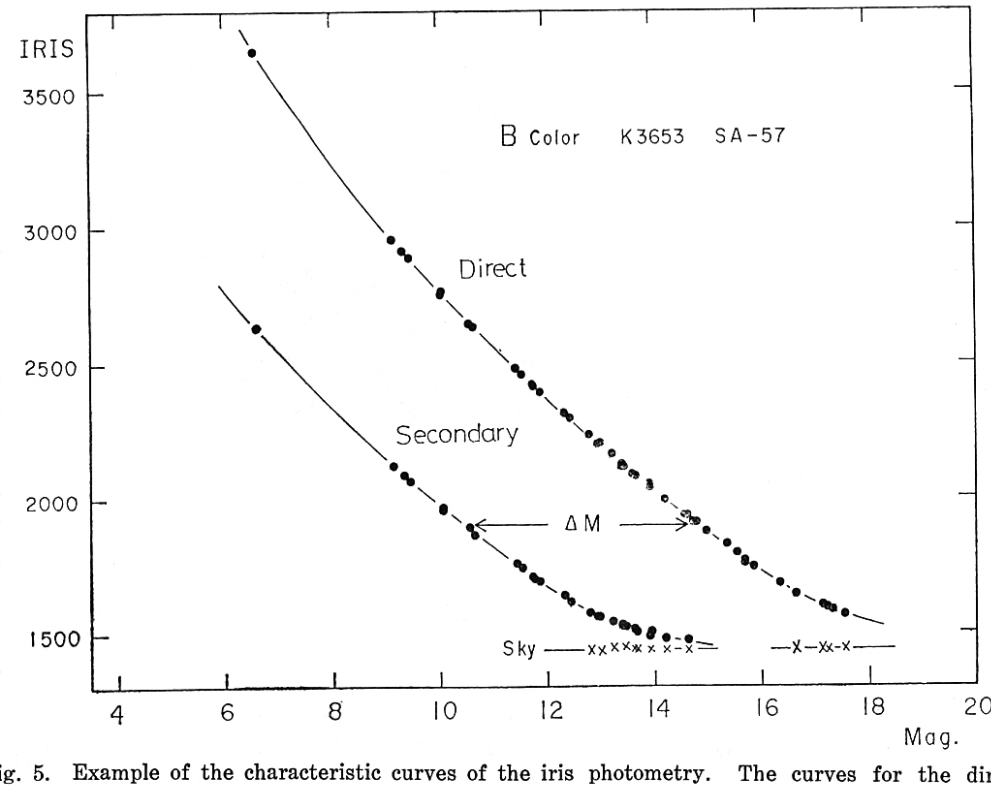

Fig. 5. Example of the characteristic curves of the iris photometry. The curves for the direct images and the secondary images are shown.

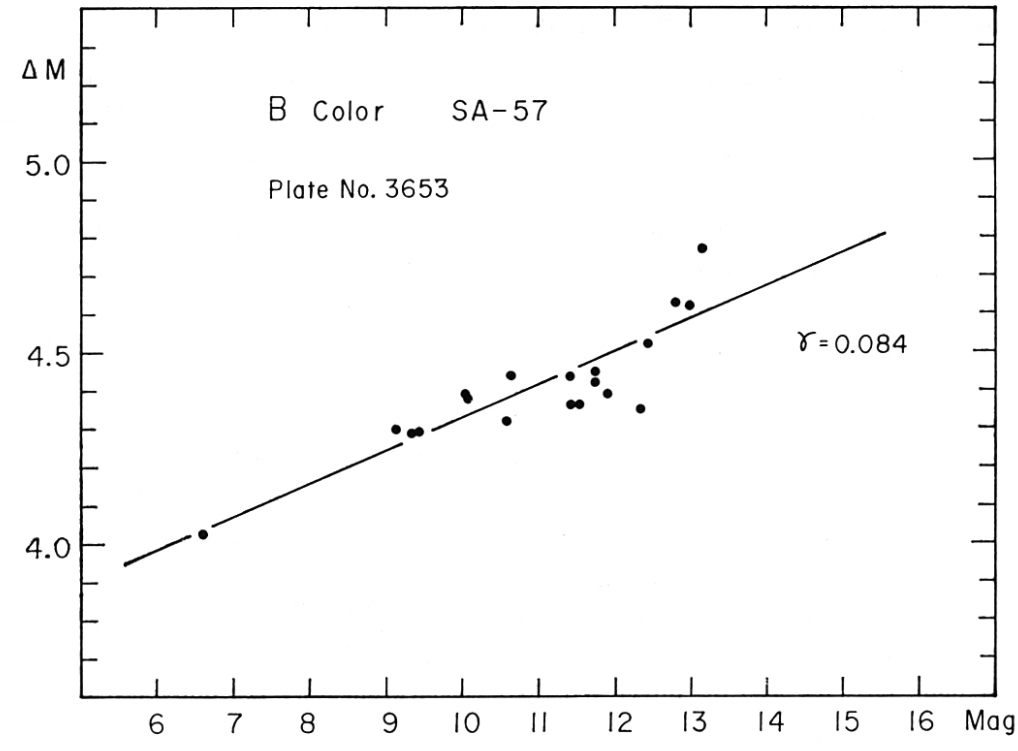

Fig. 6. The magnitude difference between the direct and secondary images plotted against the magnitudes of the standard stars. The straight line has a slope of 0.084, which is fitted by the least squares method.

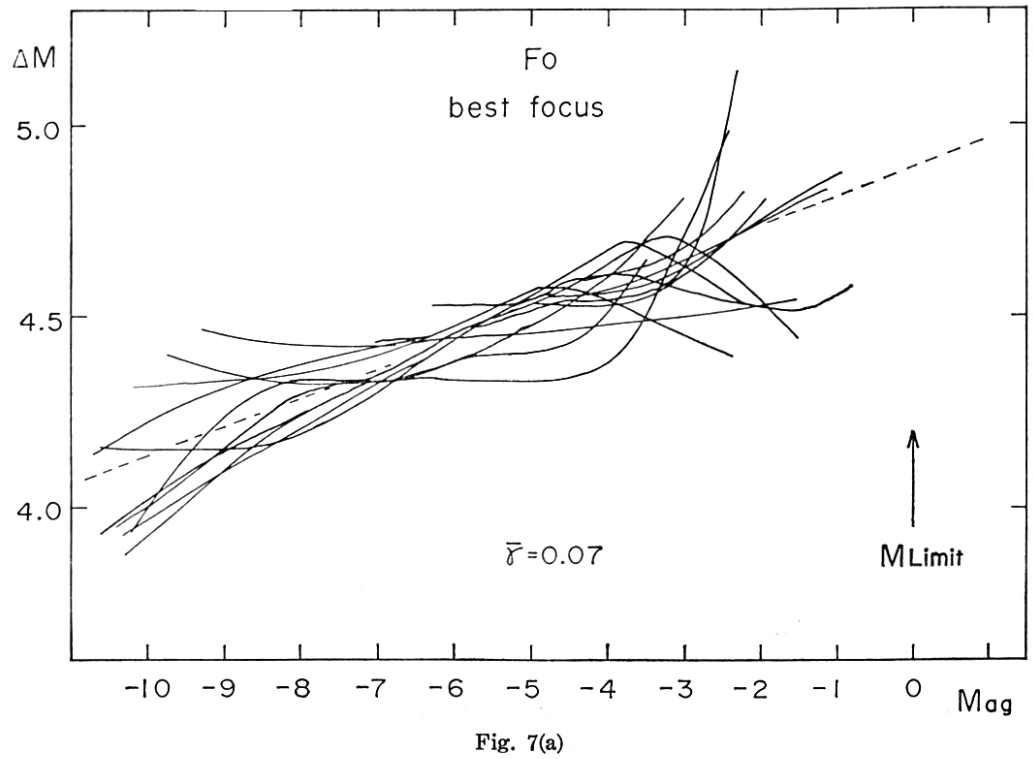

Fig. 7(a)

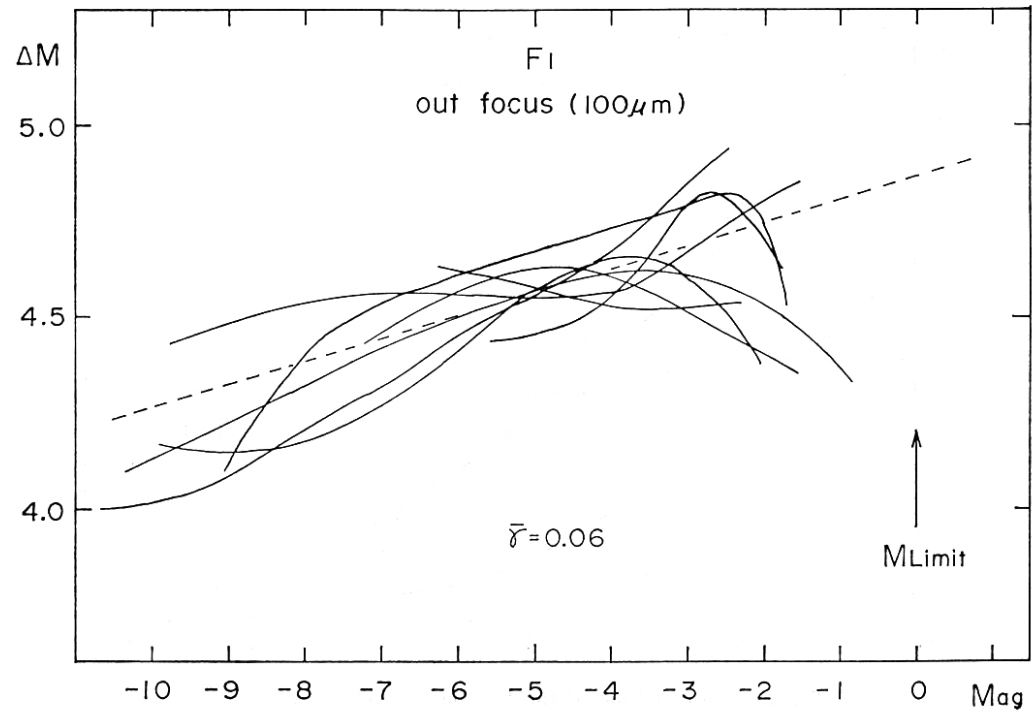

Fig. 7(b)

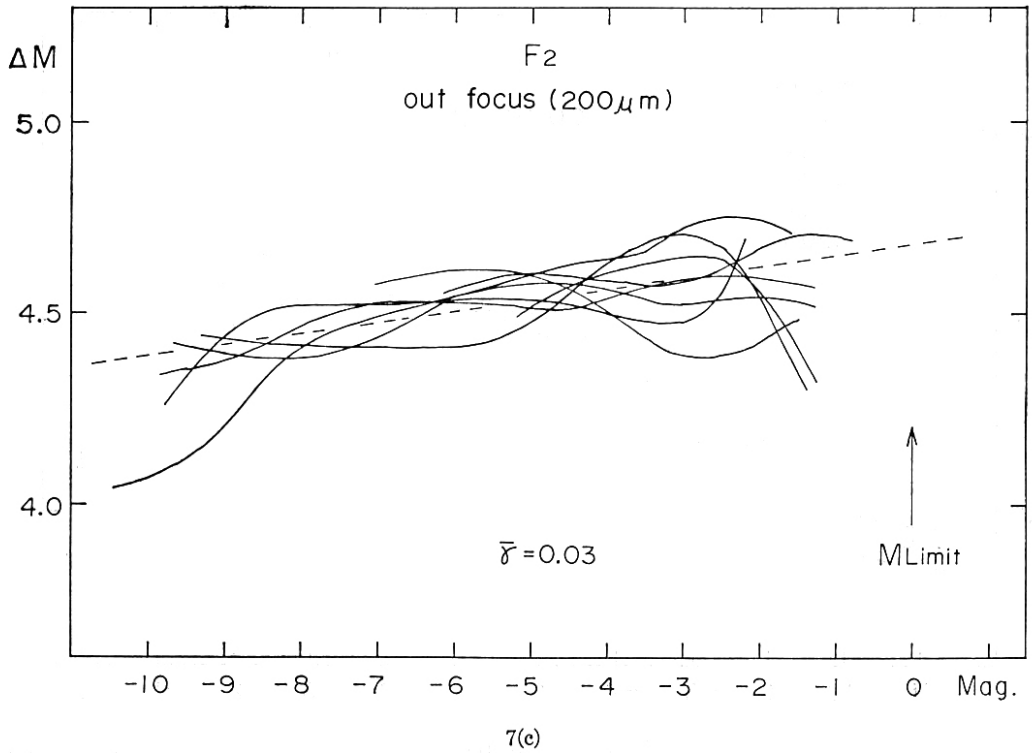

7(c)

Fig. 7. The magnitude differences in a various artificial seeing conditions; (a) in-focus, (b) out-of-focus by 100 μm, and (c) out-of-focus by 200 μm. The systematic magnitude dependence is most obvious in the in-focus plates.

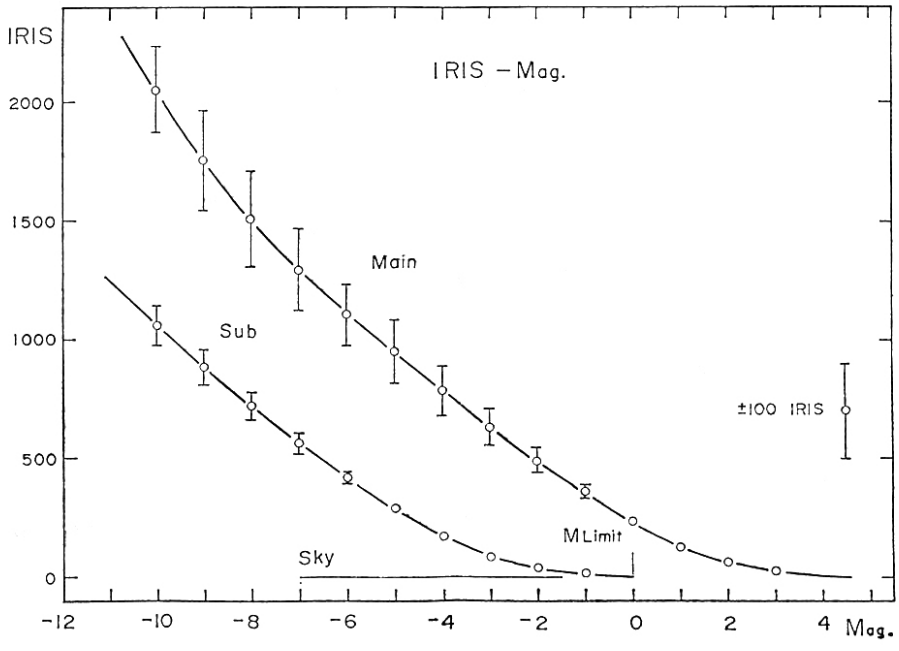

Fig. 8. The definition of the limiting magnitude, M_{Limit}.

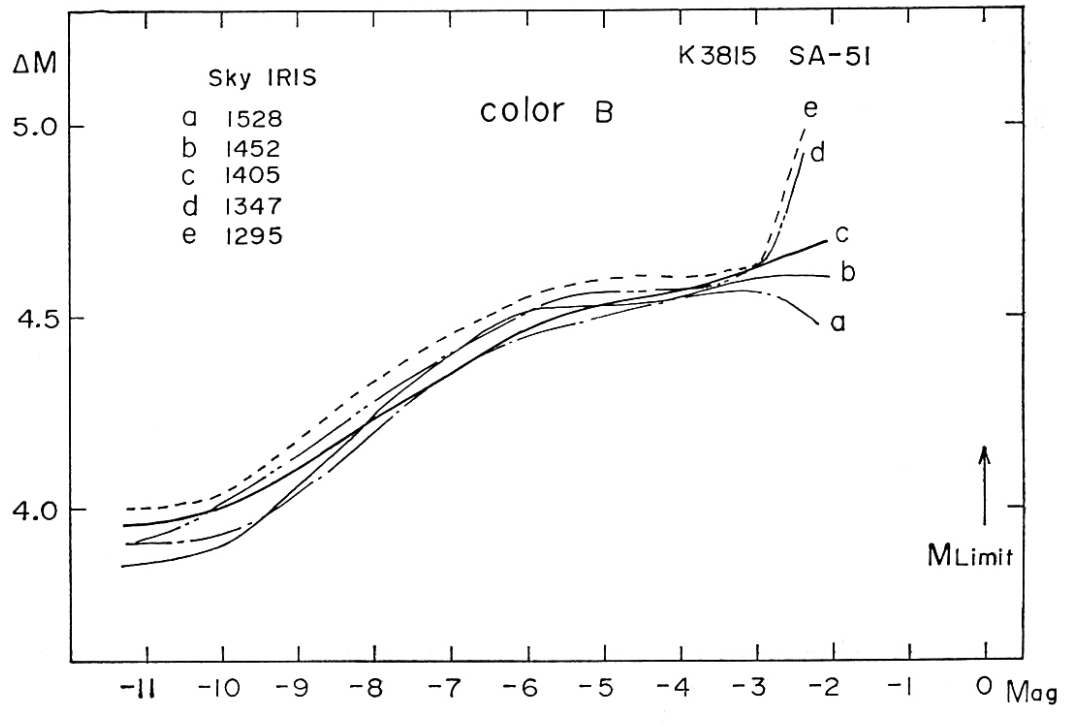

Fig. 9. Variation of the magnitude difference due to the change in the iris value at the sky level. In this case, the value of 1400 is the optimum iris value at the sky level on the plate.

various artificial seeing conditions, i.e., in-focus and out-of-focus by 100 μm and 200 μm. These plates were measured with the iris photometer and the results are shown in figures 7(a)–7(c). The difference of the exposure time should be taken into account in comparing ΔM versus magnitude relation for different plates, since the image of a star on the plate can be somewhat bright or very faint depending upon the exposure time. For the purpose of normalizing the difference of exposure time, we introduce a quantity, M_{Limit}, which is defined for each plate by the magnitude where the characteristic curve for the secondary images intersects the sky level (Figure 8). The abscissa of figures 7(a)–7(c) is the magnitude relative to M_{Limit}. Figure 7 shows that in-focus plates reveals the strongest magnitude dependence, that is, the magnitude differences are smaller for brighter stars. On the other hand, the out-of-focus plates show weaker magnitude dependence. The effect of out-focusing is larger on the direct image than on the secondary image, since the F ratio is much smaller for the direct image than for the secondary image. The defocusing thus contributes to decrease the difference of image structure between the direct and the secondary image, and results in a weaker magnitude difference.

We also find little evidence that plate-to-plate variation of ΔM versus magnitude relation is correlated with the color band. Accordingly, the difference of the chromatic aberration in different color bands have little effect on the magnitude difference at least in the U, B and V bands.

It is preferable to keep the iris reading of the sky level at a constant value when measuring the plates with different sky density in order to obtain the stable results. We adjust the iris reading at the sky level to be about 1400. Figure 9 shows the effect of changing this iris value on the ΔM versus magnitude relation. It is found that a small change of the iris value within 50 around 1400 yields little effect on the magnitude difference.

5. Approximation formula of the magnitude difference.

If the single calculated value, 4.45 magnitude, is used for magnitude calibration of the secondary images, a systematic error will be introduced which is due to the magnitude dependence described in the preceding section. Thus, in order to obtain the magnitudes of the secondary images free from this systematic error we introduce a general function in the following way. We assume that the magnitude difference can be represented by a linear function of the magnitude of the standard star. The magnitude difference ΔM of the i-th standard star is expressed by

$$\Delta M_i = \gamma(M_i - M_{\text{Limit}}) + C \qquad (1)$$

where M_i is the magnitude of the standard star, M_{Limit} is the limiting magnitude of the measurement defined in section 4, and γ is the slope of the ΔM versus magnitude relation. Here, the question is how to estimate the optimum values of γ, C, and M_{Limit}.

In figure 10 the mean magnitude difference is plotted against the magnitude of standard stars, error bars showing the standard deviations. The data are obtained by averaging thirty measurements after normalizing the exposure difference using M_{Limit}. As shown in this figure, the standard deviation is smallest at the point 5 magnitude brighter than the limiting magnitude. This point is used as the reference point to estimate the parameter values C and γ. We adopt the magnitude difference at this point, 4.53 magnitude, as the constant C in equation (1).

It is found that the characteristic curve always have a simillar form for different plates and it can be represented by a single mean characteristic curve with a reasonable accuracy. The limiting magnitude M_{Limit} can be derived from the mean characteristic curve. According to our

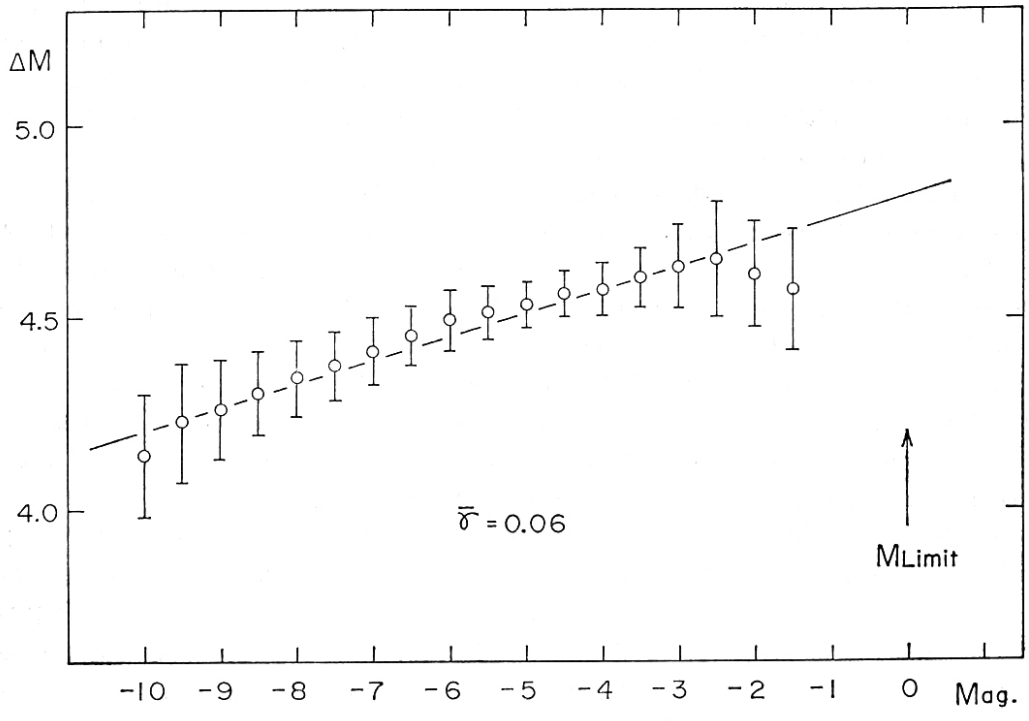

Fig. 10. The magnitude difference obtained by averaging thirty measurements.

experience, it is appropriate to adopt a value of $M_{100}+3.25$ as M_{Limit}, where M_{100} is the magnitude at the point where the iris value becomes 100 counts larger than the sky level.

Using the values of C and M_{Limit} thus derived, we can obtain the optimum value of γ by solving an equation,

$$\gamma=(4.53-\Delta M)/[(M_{\text{Limit}}-5)-M]\,. \qquad (2)$$

by means of the least squares method.

Experiments have shown that we can obtain the magnitudes of secondary images within the accuracy of 0.1 magnitude, if we use the equation (1) with the parameters obtained above.

References

Blanco, V.M. 1982, Publ. Astron. Soc. Pacific, 94, 201.
Ishida, K., Maehara, M., and Ohashi, M. 1980, Tokyo Astron. Obs. Report, 18, 260 (in Japanese).
Muller, A.B. 1980, ESO Messenger, 22, 18.
Noguchi, T. and Soyano, T. 1982, Tokyo Astron. Obs. Report, 19, 567 (in Japanese).
Noguchi, T., Maehara, H., and Kondo, M. 1980, Ann. Tokyo Astron. Obs. 2nd Ser., 18, 55.
Noguchi, T., He, X., Cannon, R.D., Smith, M.G., Okamura, S., and Takase, B. 1983, Publ. Astron. Soc. Japan, 35, 337.
Pickering, E. 1891, Harvard Ann., 26, 14.
Purgathofer, A. 1969, Lowell Obs. Bull., 2, 98.
Racine, R. 1969, Astron. J., 74, 1073.
Soyano, T, Nishino, Y., and Noguchi, T. 1983, Tokyo Astron. Obs. Report, 20 (in press).
Takase, B. 1980, Publ. Astron. Soc. Japan, 32, 605.
Takase, B., Noguchi, T., and Maehara, M. 1983, Ann. Tokyo Astron. Obs., 2nd Ser., 19, No. 3 (in press).
Takase, B., Ishida, K., Shimizu, M., Maehara, H., Hamajima, K., Noguchi, T., and Ohashi, M. 1977, Ann. Tokyo Astron. Obs., 2nd Ser., 16, 74.